The development of 4-channel Fourier transform polarization spectrometer

Citation for published version:
Zhao, J & Wang, W 2017, The development of 4-channel Fourier transform polarization spectrometer. in C Zhang & A Asundi (eds), *Second International Conference on Photonics and Optical Engineering.*, 1025641, Proceedings of SPIE, vol. 10256, SPIE. https://doi.org/10.1117/12.2257881

Digital Object Identifier (DOI):
10.1117/12.2257881

Link:
Link to publication record in Heriot-Watt Research Portal

Document Version:
Peer reviewed version

Published In:
Second International Conference on Photonics and Optical Engineering

The development of 4-channel Fourier transform polarization spectrometer

Juan Zhao[a,b,c], Wei Wang[a]*
[a] Institute of Photonics and Quantum Sciences, School of Engineering and Physical Science, Heriot-Watt University, Edinburgh, United Kingdom, EH14 4AS
[b] SuperD Co., Ltd., Nanshan district, Shenzhen, China, 518057
[c] College of Applied Sciences, Beijing University of Technology, Beijing, China, 100124

ABSTRACT

A 4-channel Fourier transform polarization spectrometer is conceptually proposed and experimentally demonstrated as an extension of the conventional Fourier transform spectrometer for scalar spectra collection. The design consists of a typical Michelson interferometer and four sets of polarizer arrays inserted into the incident light path, two interference arms and an output light path, respectively. This novel device facilitates the measurement of all elements in the coherence tensor of a radiative source simultaneously. As an extension of the Wiener-Khintchine theorem, the four sets of spectra with polarization information can be recovered by applying Fourier transforms to the recorded sets of interferograms. The reconstructed polarization spectra have been displayed on a Poincare sphere to demonstrate how a light source emits radiation at each wavelength with different polarization information. The proposed Fourier transform polarization spectrometer provides a new opportunity to identify unknown birefringent materials and determine the quality and content of a birefringent sample for material analysis.

Keywords: Polarization, spectrometer, interferometer, Fourier analysis, coherence.

1. INTRODUCTION

In the history of optics, the subjects of coherence and polarization have been developed independently. Coherence arises from correlation between fluctuations at two different time or space points. Polarization is a fluctuating components of the electric field at a single point. When we discuss the coherence properties of the field, some simplified models have been used by treating the optical field by ignoring their polarization properties [1-3]. Especially, the conventional Fourier transform spectroscopy which the spectrum is reconstructed from a Fourier transform of temporal coherence of light that doesn't take into account the polarization arising from the vector nature of the electromagnetic field [4]. However, effective methods for description of both polarization and spectrum are urgent needed [5-8].

Recently, a unified theory of polarization and coherence was achieved [3,9,10]. The second order correlation properties of an electric field can be characterized by a 2×2 electric spectral density matrix. If we can get this matrix, then we'll be able to completely describe their coherence and polarization properties for an electromagnetic beam.

In this paper, we introduce the electric Wiener-Khintchine theorem for stochastic electromagnetic fields firstly. Then, we propose a novel Fourier transform polarization spectrometer which can be used to measure electric spectral density matrix. Finally, we reconstruct polarization and spectrum of electromagnetic fields by using the proposed optical system.

*w.wang@hw.ac.uk Tel: +44 (0) 131 451 3141; Fax: +44 (0) 131 451 3129

2. PRINCIPLE

2.1 Michelson interferometer and the Wiener-Khintchine theorem

We begin by briefly recalling the Michelson interferometer, the spectral density and the Wiener-Khintchine theorem in scalar description.

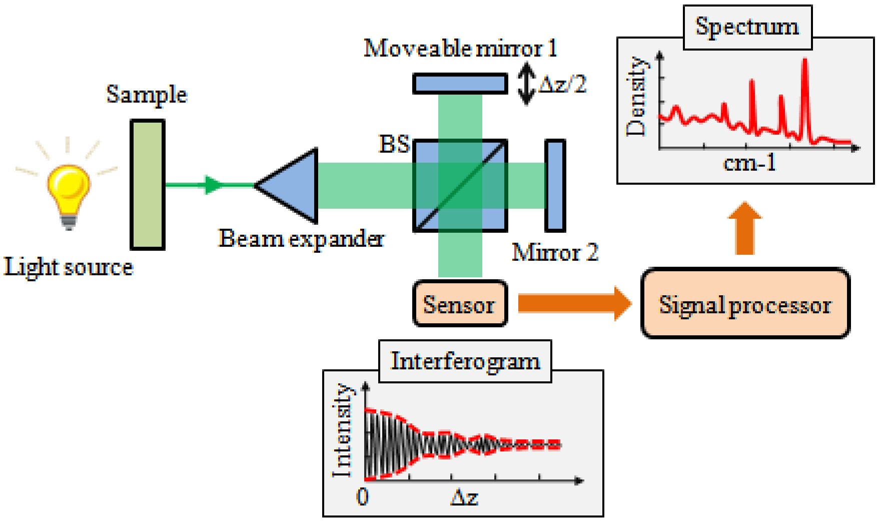

Figure 1. Typical Fourier transform spectrometer.

Consider the conventional Fourier transform spectrometer illustrated in figure 1, the Michelson interferometer is used to measure the wavelength of incident light. In this setup, light from broadband source passes through a sample and collimated by beam expander lens. The collimated beam is split into two arms by beam splitter BS, reflected back from separate mirrors, recombined at the BS, and projected on an image sensor. If the optical path difference of the two beams is not too much, an interference pattern is produced. When mirror 1 is moved, a relative time delay $\tau = \Delta z / c$ is introduced between the two interfering beams, the interference pattern on the screen changes. The intensity incident on the sensor can be written as

$$I(\tau) = \left\langle \left| K_1 \boldsymbol{E}(t) + K_2 \boldsymbol{E}(t+\tau) \right|^2 \right\rangle = (K_1^2 + K_2^2) I_0 + 2 K_1 K_2 \operatorname{Re}\left\{ \Upsilon(\tau) \right\}, \tag{1}$$

where K_1 and K_2 are the losses in the two interference beams, $\boldsymbol{E}$ is complex optical field of the incident light, I_0 is defined as

$$I_0 = \left\langle \left| \boldsymbol{E}(t) \right|^2 \right\rangle = \left\langle \left| \boldsymbol{E}(t+\tau) \right|^2 \right\rangle \tag{2}$$

and

$$\Upsilon(\tau) = \left\langle \boldsymbol{E}^*(t) \boldsymbol{E}(t+\tau) \right\rangle \tag{3}$$

is the autocorrelation (self-coherence function) of the optical field. The asterisk denotes the complex conjugate, and the angular bracket indicates a time average. A typical interferogram I with intensity plotted against mirror displacement Δz from the position of equal path length is shown in figure 1, the envelope of the fringe pattern is drawn dotted. The self-coherence function $\Upsilon(\tau)$ can be measured from the visibility of observed fringes.

Here, we introduce the definition of the power spectral density (or spectrum) of the beam

$$\boldsymbol{S}(\omega) = \frac{1}{2\pi} \int_{-\infty}^{\infty} \Upsilon(\tau) \exp(j\omega\tau) d\tau , \tag{4}$$

Eq. (4) is known as the Wiener-Khintchine theorem: the spectrum $\boldsymbol{S}(\omega)$ of a light and its self-correlation $\boldsymbol{\Upsilon}(\tau)$ form a Fourier transform pair [1-3]. We have seen that the power spectral density (spectrum) of the light can be completely determined if the interferogram is observed.

2.2 Electric Wiener-Khintchine theorem for stochastic electromagnetic fields

In vector field, the self-correlation of a stochastic electromagnetic beam is conveniently described by a 2×2 matrix, called as electric self-coherence tensor:

$$\mathbf{\Gamma}(\tau) \equiv \left[\boldsymbol{\Gamma}_{\alpha\beta}(\tau)\right] = \begin{bmatrix} \left\langle \boldsymbol{E}_x^*(t)\boldsymbol{E}_x(t+\tau)\right\rangle & \left\langle \boldsymbol{E}_x^*(t)\boldsymbol{E}_y(t+\tau)\right\rangle \\ \left\langle \boldsymbol{E}_y^*(t)\boldsymbol{E}_x(t+\tau)\right\rangle & \left\langle \boldsymbol{E}_y^*(t)\boldsymbol{E}_y(t+\tau)\right\rangle \end{bmatrix}, \tag{5}$$

where, α and β denote the subscripts x or y, respectively. $\boldsymbol{E}_x$ and $\boldsymbol{E}_y$ are the components of the complex electric field vector, represented by analytic signals in two mutually orthogonal directions perpendicular to the axis of the beam. The counter-diagonal elements of the matrix $\left\langle \boldsymbol{E}_x^*(t)\boldsymbol{E}_y(t+\tau)\right\rangle = \left\langle \boldsymbol{E}_y^*(t)\boldsymbol{E}_x(t+\tau)\right\rangle^*$.

Here, we introduce the spectral polarization tensor $\mathbf{W}(\omega)$ as the Fourier transform of the electric self-coherence tensor $\mathbf{\Gamma}(\tau)$ of the electric field, that is the electric Wiener-Khintchine theorem [3]

$$\mathbf{W}(\omega) = \frac{1}{2\pi}\int_{-\infty}^{\infty} \mathbf{\Gamma}(\tau)\exp(i\omega\tau)d\tau\ . \tag{6}$$

For stochastic electric fields, the spectral polarization tensor may also be expressed as a correlation matrix,

$$\mathbf{W}(\omega) \equiv \left[\boldsymbol{W}_{\alpha\beta}(\omega)\right] = \begin{bmatrix} \left\langle \boldsymbol{E}_x^*(\omega)\boldsymbol{E}_x(\omega)\right\rangle & \left\langle \boldsymbol{E}_x^*(\omega)\boldsymbol{E}_y(\omega)\right\rangle \\ \left\langle \boldsymbol{E}_y^*(\omega)\boldsymbol{E}_x(\omega)\right\rangle & \left\langle \boldsymbol{E}_y^*(\omega)\boldsymbol{E}_y(\omega)\right\rangle \end{bmatrix}, \tag{7}$$

where, the counter-diagonal elements of the matrix $\left\langle \boldsymbol{E}_x^*(\omega)\boldsymbol{E}_y(\omega)\right\rangle = \left\langle \boldsymbol{E}_y^*(\omega)\boldsymbol{E}_x(\omega)\right\rangle^*$.

2.3 Determination of the spectral polarization tensor from experiments

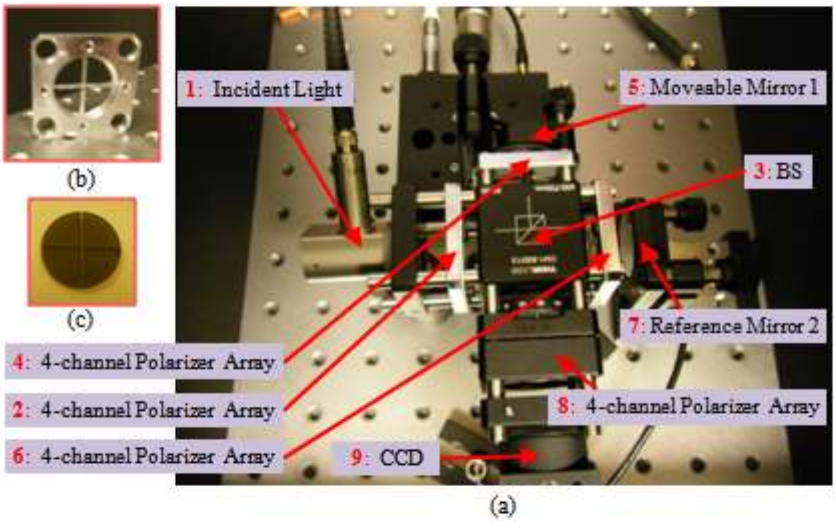

Figure 2. (a) 4-channel Fourier transform polarization spectrometer, (b) 4-channel polarizer array holder, (c) Sub-linear polarizers.

So far we have introduced the electric Wiener-Khintchine theorem as shown in Eq. (6). If we want to characterize the spectral polarization tensor, we have to modify the Michelson interferometry system. As shown in Figure 2, the experimental setup consists of a typical Michelson interferometer and 4 sets of polarizer arrays. The 4 sets of polarizer arrays are placed in incident light path, two interference arms and output light path, respectively, each polarizer array has one or more sub- linear polarizers. This device not only have the advantages of measuring all of the elements in the electric self-coherence tensor, but also are favorable to the scalar spectrum analysis, what follows is more detail about how and why it works.

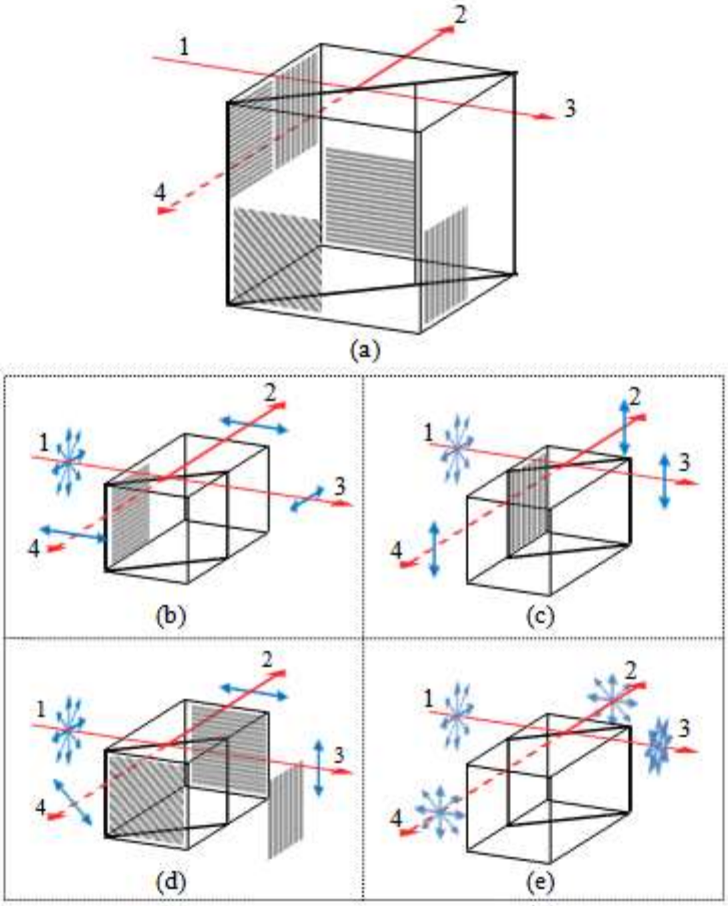

Figure 3. Four channels beam splitter cube. (a) Structural diagram, (b-e) Functional decomposition diagrams.

Consider the 4-channel beam splitter cube illustrated in Figure 3(a). We have inserted 4 polarizer arrays into the incident light path (path 1), two interference arms (path 2,3) and an output light path (path 4), respectively. As seen in decomposition diagram (b), the first channel is used to detect the interference between two horizontally polarized beams $\left\langle \boldsymbol{E}_x^*(t)\boldsymbol{E}_x(t+\tau)\right\rangle$. In Fig.3(c), the second channel corresponds to an interferogram from two vertically polarized beams $\left\langle \boldsymbol{E}_y^*(t)\boldsymbol{E}_y(t+\tau)\right\rangle$. In Fig.3 (d), the third channel corresponds to an interferogram from two orthogonally polarized beams $\left\langle \boldsymbol{E}_y^*(t)\boldsymbol{E}_x(t+\tau)\right\rangle$. To observe the polarization fringes generated from the interference between $\boldsymbol{E}_x$ and $\boldsymbol{E}_y$ components on viewing screen, we have inserted a 45° linear polarizers in the output light path to shift polarization direction. In Fig.3 (e), the fourth channel corresponds to the scalar interference $\left\langle \boldsymbol{E}^*(t)\boldsymbol{E}(t+\tau)\right\rangle$ that is used for performance comparisons. Therefore, the electric self-coherence tensor $\boldsymbol{\Gamma}(\tau)$ and scalar self-correlation $\boldsymbol{\Upsilon}(\tau)$ can be examined in one test (see Figure 4).

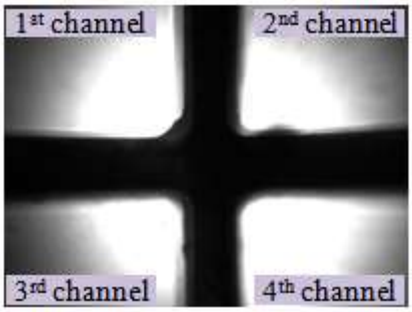

Figure 4. Image array on the CCD sensor: the 1st channel corresponds to $\boldsymbol{\Gamma}_{xx}(\tau)$; the 2nd channel corresponds to $\boldsymbol{\Gamma}_{yy}(\tau)$; the 3rd channel corresponds to $\boldsymbol{\Gamma}_{yx}(\tau)$; the 4th channel corresponds to $\boldsymbol{\Upsilon}(\tau)$.

2.4 Spectral Stokes parameters and Poincare sphere

Instead of characterizing the properties of stochastic electromagnetic field by the 2×2 matrix, spectral Stokes vector has been introduced [3]

$$S(\omega) \equiv \left(S_0(\omega), S_1(\omega), S_2(\omega), S_3(\omega)\right). \tag{8}$$

The spectral stokes parameters and the elements of the spectral polarization tensor are related by the formulas

$$\begin{aligned} S_0(\omega) &= \boldsymbol{W}_{xx}(\omega) + \boldsymbol{W}_{yy}(\omega), \\ S_1(\omega) &= \boldsymbol{W}_{xx}(\omega) - \boldsymbol{W}_{yy}(\omega), \\ S_2(\omega) &= \boldsymbol{W}_{xy}(\omega) + \boldsymbol{W}_{yx}(\omega) = 2\,\mathrm{Re}\left\{\boldsymbol{W}_{xy}(\omega)\right\}, \\ S_3(\omega) &= i\left[\boldsymbol{W}_{yx}(\omega) - \boldsymbol{W}_{xy}(\omega)\right] = 2\,\mathrm{Im}\left\{\boldsymbol{W}_{xy}(\omega)\right\}. \end{aligned} \tag{9}$$

We can readily to see $S_0(\omega) = S(\omega)$, that is to say the 4th channel signal corresponds to $S_0(\omega)$.

The spectral Stokes parameters can be visualized using a Poincare sphere, as shown in Figure 5. The radius of the sphere is $S_0(\bar{\omega})$, the coordinates of the vector is (S_1, S_2, S_3), and color of the vector represents its wavelength (or spectrum) $\lambda = 2\pi c/\omega$. The four-dimensional data (S_1, S_2, S_3, ω) in the Poincare sphere are able to demonstrate how a light source emits radiation at each wavelength with different polarization information.

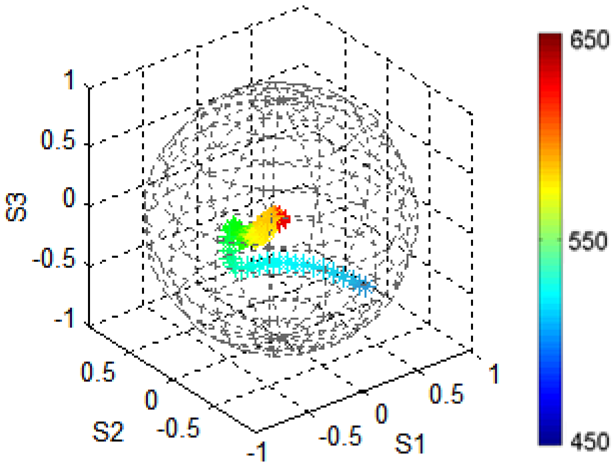

Figure 5. Poincare sphere with a color bar.

3. EXPERIMENTS AND RESULTS

The experiment setup has been shown in Figure 2. The light source in our experiment is a red GaAIAs LED with peak wavelength 660nm and spectrum half width 20nm. The original light emitting from LED is a non-polarization beam. Some polarization optics have been placed behind the light source to serve as stochastic electromagnetic light source. For example, a single linear polarizer may generate a linear polarization beam, a linear polarizer with a quarter-wave plate may generate a circular polarization beam, and a linear polarizer with a depolarizer may generate a partially polarized beam. These optics can only reorganize polarization properties of the incident light; they does not change the spectrum.

Interferogram arrays have been detected by CCD. As shown in Figure 6, (a)-(d) are interferogram arrays of non-polarization light, linear polarization light, circular polarization light and partially polarized light, respectively. After DC parts of interferogram have been removed, the amplitude of each element in electric self-coherence tensor $\left\langle \boldsymbol{E}_{\alpha}^{*}(t)\boldsymbol{E}_{\beta}(t+\tau)\right\rangle$ $(\alpha, \beta = x, y)$ or scalar self-coherence function $\left\langle \boldsymbol{E}^{*}(t)\boldsymbol{E}(t+\tau)\right\rangle$ can be obtained.

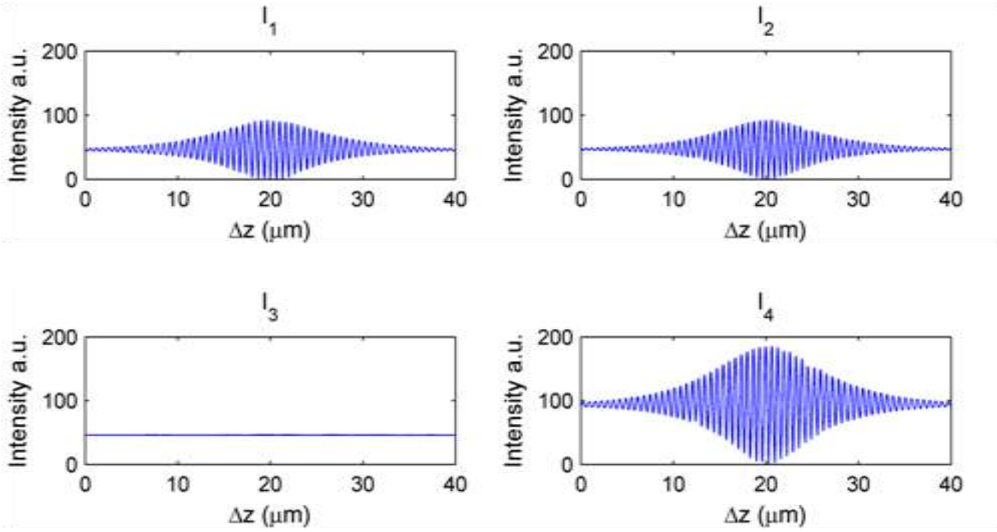

(a)

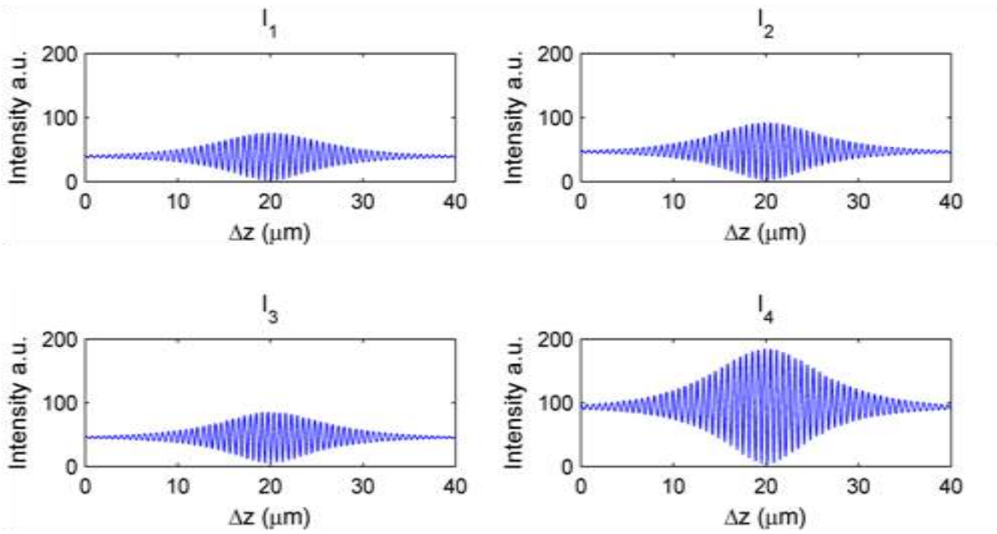

(b)

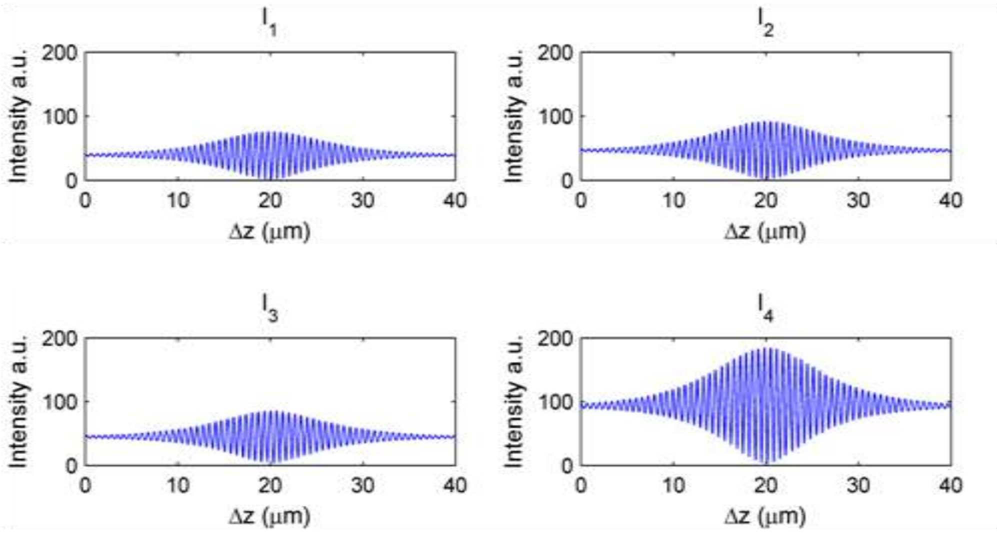

(c)

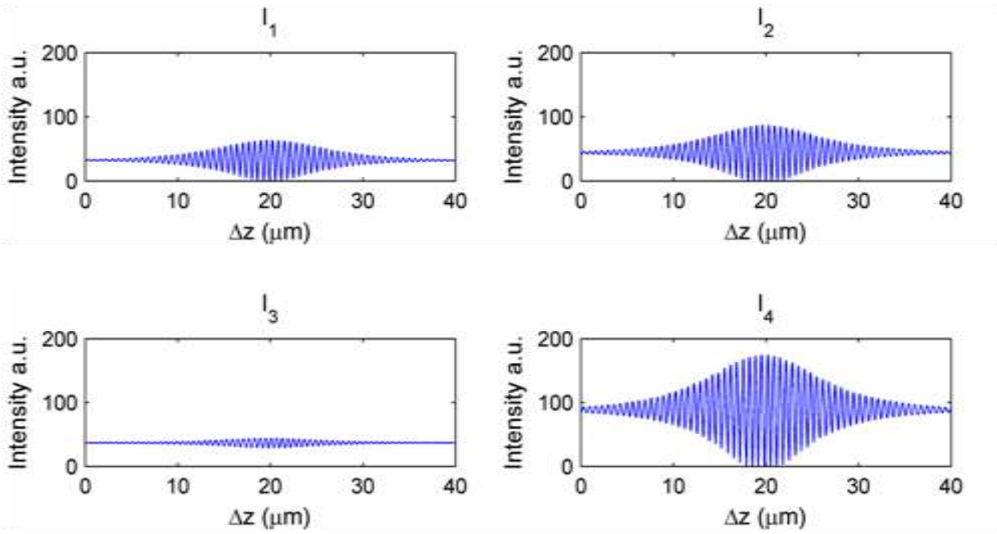

(d)

Figure 6. Four-channel interferograms recorded by CCD. (a) Non-polarization light, (b) Linear polarization light, (c) Circular polarization light, (d) Partially polarized light.

Now, we calculate spectrum by using Fourier analysis (Eq. 4 and Eq. 6) and show the scalar spectrum with 2D curves (see Figure7) and the polarization spectrum with Poincare spheres (see Figure8). By comparing these two graphs, we find that the polarization spectrum has a better ability to identify different types of signals, especially, when the scalar spectrums of substances are similar, polarization information becomes an important criterion to distinguish them.

The purpose of these experiments is to demonstrate some basic functions of our system. We have only used a narrow band light source to obtain some spectral maps which are similar to Gauss functions. However, our system is not limited to narrow band light source, the Fourier transform polarization spectrometer is also suitable for wide band spectrum acquisition. In the same way, we might obtain both polarization spectrum and scalar spectrum after a single shot.

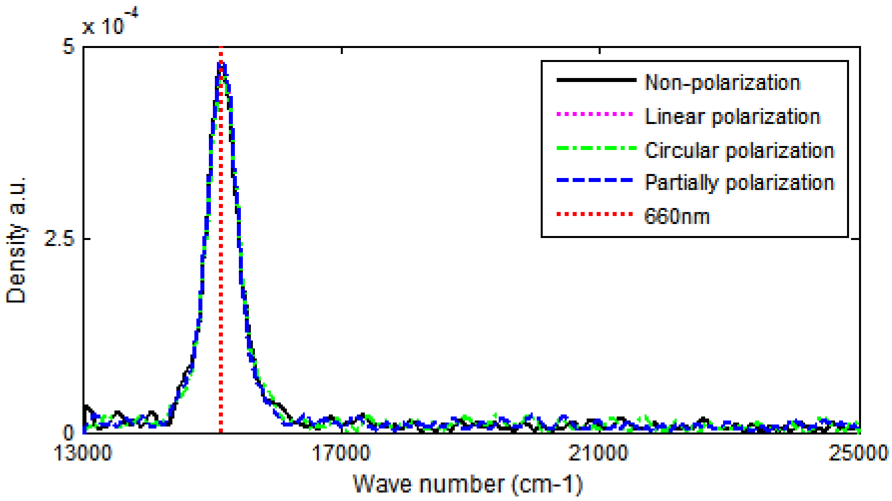

Figure 7. Scalar spectrum. The peak wavelength is 660nm and spectrum half width is 20nm.

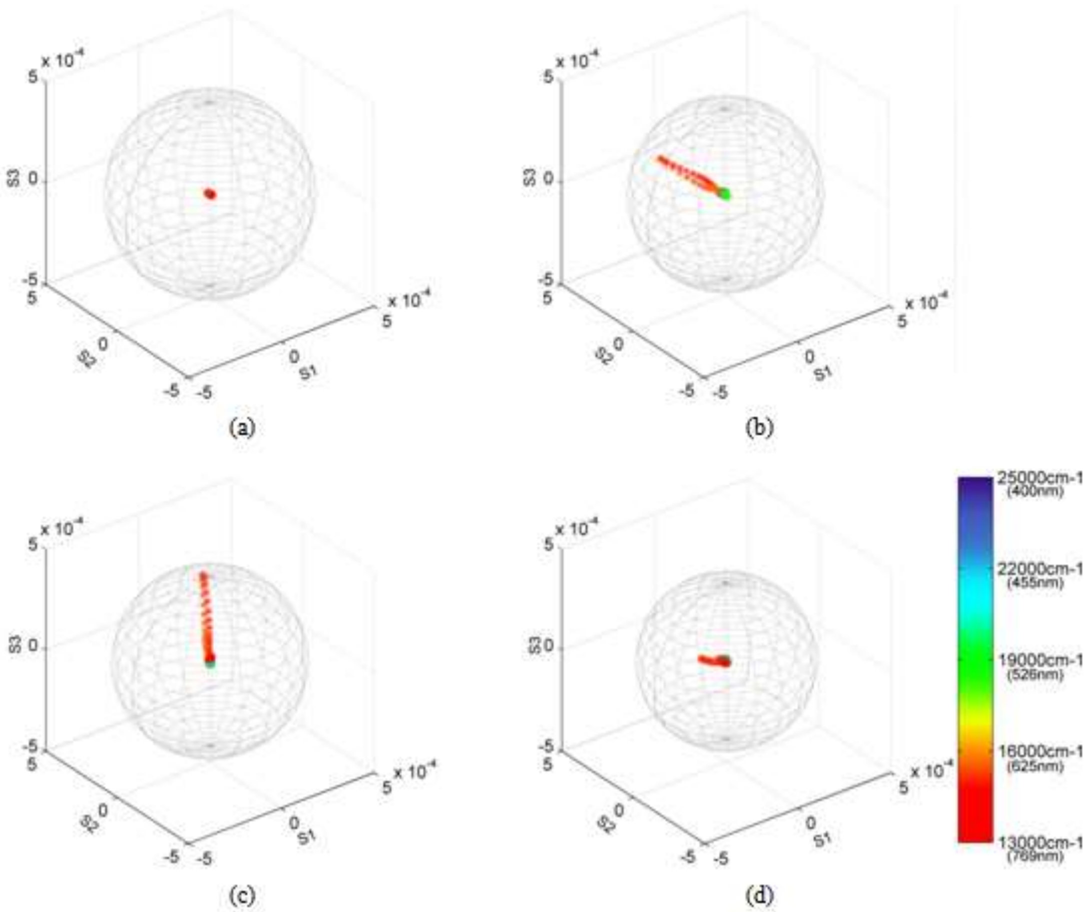

Figure 8. Polarization spectrum. (a) Non-polarization light, (b) Linear polarization light, (c) Circular polarization light, (d) Partially polarized light.

4. CONCLUSIONS

In this paper, we have extended the Wiener-Khintchine theorem into vectorial domain, and introduced a 4-channel Fourier transform polarization spectrometer. Finally, we have calculated spectrum by using Fourier analysis and show the spectral polarization tensor with a 4D Poincare sphere and the scalar spectrum with a 2D curve. By comparing the two graphs, we find that the polarization spectrum has a better ability to identify different types of signals, especially, when the scalar spectrums of substances are similar, polarization information becomes an important criterion to distinguish them. The proposed Fourier transform polarization spectrometer provides a new opportunity to identify unknown birefringent materials and determine the quality and content of a birefringent sample for material analysis.

ACKNOWLEDGMENTS

We are thankful to Prof. Steen G. Hanson and Dr. Michael L. Jakobsen of Technical University of Denmark, Prof. Mitsuo Takeda of Utsunomiya University for their helpful discussion. Part of this research was supported by the EPSRC (EP/K031643/1) and the SUPA START under grant no. SSG040. J. Zhao acknowledges financial support from the Scottish Overseas Research Student Awards Scheme (SORSAS), Guangdong Innovative & Entrepreneurial Research Team Program and the Shenzhen Peacock Program.

REFERENCES

[1] J. W. Goodman, [Statistical Optics], John Wiley & Sons Inc., Chap.5 (2000).
[2] M. Born, E. Wolf, [Principles of Optics], Cambridge University Press, Chap.10 (1980).
[3] E. Wolf, [Introduction to the Theory of Coherence and Polarization of Light], Cambridge University Press, Chap.2 and Chap.9 (2007).
[4] R.J. Bell, [Introductory Fourier Transform Spectroscopy], New York Academic Press (1972)
[5] X. Steve Yao, Bo Zhang, Xiaojun Chen, Alan E. Willner, "Real-time optical spectrum analysis of a light source using a polarimeter," Optics Express 16, 17854-17863 (2008)
[6] Chris T. Middleton, David B. Strasfeld, Martin T. Zanni, "Polarization shaping in the mid-IR and polarization-based balanced heterodyne detection with application to 2D IR spectroscopy," Optics Express 17, 14526-14533 (2009)
[7] Mohammad Neshat, N. P. Armitage, "Terahertz time-domain spectroscopic ellipsometry: instrumentation and calibration," Optics Express 20, 29063-29075 (2012)
[8] A. L. Fymat, "Polarization Effects in Fourier Spectroscopy. I: Coherency Matrix Representation," Applied Optics 11, 160-173 (1972)
[9] E. Wolf, "Unified theory of coherence and polarization of random electromagnetic beams," Phys. Lett. A 312, 263-267 (2003).
[10] E. Wolf, "Correlation-induced changes in the degree of polarization, the degree of coherence, and the spectrum of random electromagnetic beams on propagation," Opt. Lett. 28, 1078-1080 (2003).